CALCULATION OF THE PROFILE OF THE CORONAL LINE λ171 FE IX IN THE EMISSION SPECTRUM OF SLOW MAGNETO-SONIC WAVES PROPAGATING IN THE SOLAR CORONA. 1. THE CASE OF CONSTANT DENSITY.

S. H. Mamedov [a], ***J. M. Kuli-zade*** [a], ***Z. F. Alieva*** [b], ***K. I. Alisheva*** [b*]

[a] *Shamakhy Astrophysical Observatory named after N.Tusi, Azerbaijan National Academy of Sciences, Shamakhy region, Azerbaijan*

[b] *Baku State University*

The line profiles λ 171 Å Fe IX in the emission spectrum of slow magneto-sonic waves propagating in coronal loops are calculated for an optically thin layer and constant density cases. The line profiles were calculated at the following parameter values: the amplitude of the velocity at the wave $\nu_0 = 10$ km/s, the coronal loop width 2000 km and 5000 km, the wavelength $\Lambda = 20{,}000$ km and 50,000 km, the Doppler width $\Delta\lambda_d = 0.01$Åand also at the values of sight angle and various phases of the wave. It is shown that the energy flux density and the values of the Doppler width strongly depend on the angle z and the phase of the wave.

Keywords: Line profiles–solar corona–coronal spectral lines–magneta sonic waves

1. INTRODUCTION

The research of MHD waves in coronal structures has excellent importance in coronal seismology. These waves can play a significant role in the corona's heating; besides, investigating these waves make it possible to study the solar corona's physical structure. Slow magneto-sonic waves are considered one of the candidates of heating the solar corona: these waves are generated in the photosphere as a p-mode, penetrate the corona without being reflected, are damped by the heat conduction mechanism, and consequently, can heat the corona.

* E-mail: sabirshao5@gmail.com

MHD waves in the corona were studied mainly from a theoretical point of view until the 90s of the last century. In the early 2000s, intensive extra-atmospheric observations of these waves in the corona spectrum's UV region was begun. Information about these problems could be found in the review articles [1–6]. In the present paper, the λ171 Fe IX line profile in the spectrum of slow magneto-sonic waves propagating into coronal loops is calculated. Observations of these waves are often carried out in the indicated line [6].

Let us give the observed values of the physical parameters of slow magneto-sonic waves: the propagation velocity - 25-200 km/s, the amplitude of the intensity oscillations -0,7-14,6%, the oscillation period - 145-550 s [6], the energy density flux: 313 - 610^6 [7, 8] erg sm^{-2} s^{-1}

It should be noted that in the chromosphere and corona, Doppler shift's velocities are almost an order of magnitude less than the values of non-thermal velocities found by the Doppler widths [9].

2. DERIVATION OF THE EXPRESSION FOR THE SPECTRAL LINE PROFILE

Our task - calculating the emission line profile emanating from the coronal loop along the line of sight - LZ, making an angle θ with the loop axis. As far as we know from the literature, the spectral emission line profiles in the spectrum of slow magneto-sonic waves propagating in coronal structures were not calculated.

Let us assume that the coronal loop is optically thin and that the density does not change on the wave (in the following paper, we plan to consider the case with a changing density).

The emission profile of every elementary volume along the angle of sight is Doppler, with the Doppler width $\Delta\lambda_d$, which we accept constant along the line of sight.

Fig. 1 shows the diagram of propagation of slow magneto-sonic wave inside the coronal loop with diameter H on the direction of the X-axis of the XY coordinate system, the origin of which is located in the zero phases of the considered wave; the X and Y axes are located along and perpendicular to the loop axis, respectively. All signs were described in the text under Fig. 1. The amount of emission emanating from elementary volume dl·1sm^2 located at distance l from the surface of the coronal loop, transmitting to the wavelength $\delta\lambda$ from the center of the line, is:

$$di = (\Delta\lambda) = i_0 \exp\left[-\left(\frac{\Delta\lambda - \frac{\nu l}{c}\lambda)}{\Delta\lambda_d}\right)^2\right] dl \qquad (1)$$

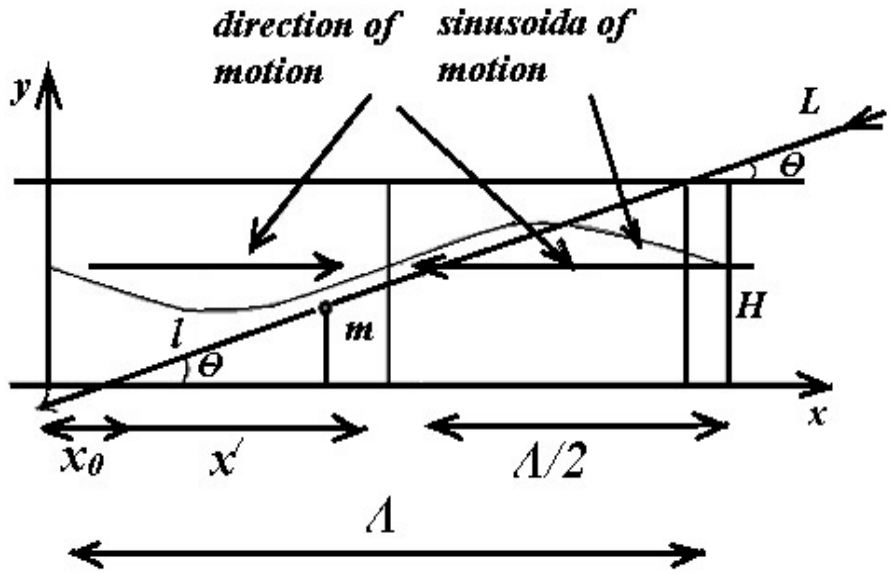

Fig. 1. Scheme of propagation of a slow magneto-sonic wave in a coronal loop; here H - the loop diameter, Λ - the sonic wavelength, L_s - the line of sight, θ - the angle between the line of sight and the direction of the loop axis, x_0 - the distance from the point of the zero phase of the wave (this point is also the origin of the coordinate system) to the intersection of the line of sight with the X -axis of the coordinate system; characterizes the phase x' - the distance along the X-axis from the point of intersection of the line of sight with the X-axis to the current considered elementary volume m, l - the distance along the line of sight from the point of intersection of the line of sight with the X-axis to the to the considered current elementry volume m

Here: i_0 - central intensity of emission profile of selected elementary volume, accepted to be constant along the whole length of the line of sight, Ls ν(l) - the rate of particles on the wave at distance l, s - speed of light. Then, the emission intensity from the entire length L of the line of sight at a distance $\delta\lambda$ from the center of the emission line will be:

$$I(\Delta\lambda) = i_0 \int_0^L \exp\left[-\left(\frac{\Delta\lambda - \left(\frac{\nu l}{c}\lambda\right)}{\Delta\lambda_d}\right)^2\right] dl \qquad (2)$$

Now we need to find ν(l). Particles motion at sonic wave is occurred along wave propagation by sine law (as can be seen from Fig. 1: $x = x_0 + x'$):

$$v(x) = \nu_0 \sin\left(\frac{2\pi x}{\Lambda}\right)$$

For the lines of sight passing through the same x_0 (this magnitude approximately characterizes the wave phase), conveniently use the expression, replacing $x = x_0 + x'$, and in this case, the variable will be x'

$$\nu\left(x'\right) = \nu_0 \sin\left(\frac{2\pi\left(x_0 + x'\right)}{\Lambda}\right) \tag{3}$$

Here: ν_0 - the velocities amplitude of particles' oscillations on the wave - wavelength of propagating slow magneto-sonic wave. It is obvious that the projection of the particle velocities amplitude on the line of sight will be:

$$Further \quad \nu_{0L} = \nu_0 \cos\theta \tag{4}$$

$$\text{Then} \;\; x' = l\cos\theta \tag{5}$$

$$\nu = (l) = \nu_0 \cos\theta \sin\left[\frac{2\pi\left(x_0 + l\cos\theta\right)}{\Lambda}\right] \tag{6}$$

Putting (6) in (2), we obtain the final expression for calculating the spectral line's profile.

$$I(\Delta\lambda) = i_0 \int_0^L \exp\left[-\left(\frac{\Delta\lambda - \nu_0 \cos\vartheta \sin\left[\frac{2\pi(x_0 + l\cos\theta)}{\Lambda}\right]\frac{\lambda}{c}}{\Delta\lambda_d}\right)^2\right] dl \tag{7}$$

As can be seen from Fig. , The line of sight passes through oppositely directed motions on the wave, and therefore, to calculate the line profile, this expression is divided into two integrals for both motion sections as follows:

$$I(\Delta\lambda) = i_0 \int_0^{l_1} \exp\left[-\left(\frac{\Delta\lambda - \nu_0 \cos\vartheta \sin\left[\frac{2\pi(x_0 + l\cos\vartheta)}{\Delta}\frac{\lambda}{c}\right]}{\Delta\lambda_d}\right)^2\right] dl + \tag{8}$$

$$i_0 \int_{l_2}^{l_1} \exp\left[-\left(\frac{\Delta\lambda + \nu_0 \cos\theta \sin\left[\frac{2\pi(x_0 + l\cos\theta)}{\Lambda}\frac{\lambda}{c}\right]}{\Delta\lambda_d}\right)^2\right] dl$$

$$l_1 = \left(\frac{\Lambda}{2} - x_0\right)\sec\theta$$

$$l_2 = \left[H - \left(\frac{\Lambda}{2} - x_0\right) \operatorname{tg}\theta\right] \operatorname{cosec}\theta$$

using expression:

$$\nu_d = \frac{\int_0^L \nu(l)dl}{L}$$

We obtain magnitude of the Doppler shift:

$$\nu_{sh} = \frac{\nu_0 \Lambda}{2\pi L}\left[-\cos\left(\frac{2\pi x_0}{\Lambda} + \frac{2\pi L\cos\vartheta}{\Lambda}\right) + \cos\frac{2\pi x_0}{\Lambda}\right] \quad (9)$$

The calculation was conducted for the profile of λ171 FeIX line; in the spectrum of slow magneto-sonic waves, this line is often used by observers. Calculation was conducted for the following parameter values: ν_0=10 km/s, Λ=20 000 km and 50,000 km [10, 11], H = 2000 km and 5000 km, L=H/cosν. $\Delta\nu_d = 0.01$, this corresponds to the temperature value $T = 10^6$ and at the values of the angle of inclination of the line of sight to the direction of wave motion $\theta = 10°, 20°, 30°, 40°, 50°, 60°, 70°and\ 80°$. Calculation of the considered spectral line profile allows us to reveal how different parameter values impact the considered wave's energy flux value and the values of non-thermal and Doppler shifts. The calculation results are given in the graphs. Fig. 2 shows examples of calculated profiles.

3. RESULTS

Velocities of Doppler shifts and non-thermal motions.

Figure 6 shows the values of velocities of the Doppler shifts ν_d and non-thermal velocities v_{nt} from the angle of inclination θ for different wavelengths Λ and loop diameter H. Fig. 7 shows the values of vd and vnt for various values of the physical parameters indicated in the figure. Fig. 9 shows the dependence of non-thermal velocities on the angle of sight at the physical parameters' values indicated in the figure.

The values of the Doppler shifts v_d, obtained by the authors from observations, are inconsistent: v_d=3km/s, v_{nt}=23km/s [9], v_d=1.8-3.7 [13], v_d=0.2-1.2 [14],. v_d =0.3-0.7 [15], v_d=1.3-1.6 [16], v_d=0.3-2.5 km/s [20], v_d= 3 km/s [23]. In standing waves, the velocities of Doppler shifts are significantly higher: vd=18 km/s [17], v_d=200 km/s [21], 191 km/s [22].

In [9], some authors' data are given, in which it is shown that the values of non-thermal velocities are almost an order of magnitude higher than the velocities of Doppler shifts. It is difficult to explain the data given in [9], taking into

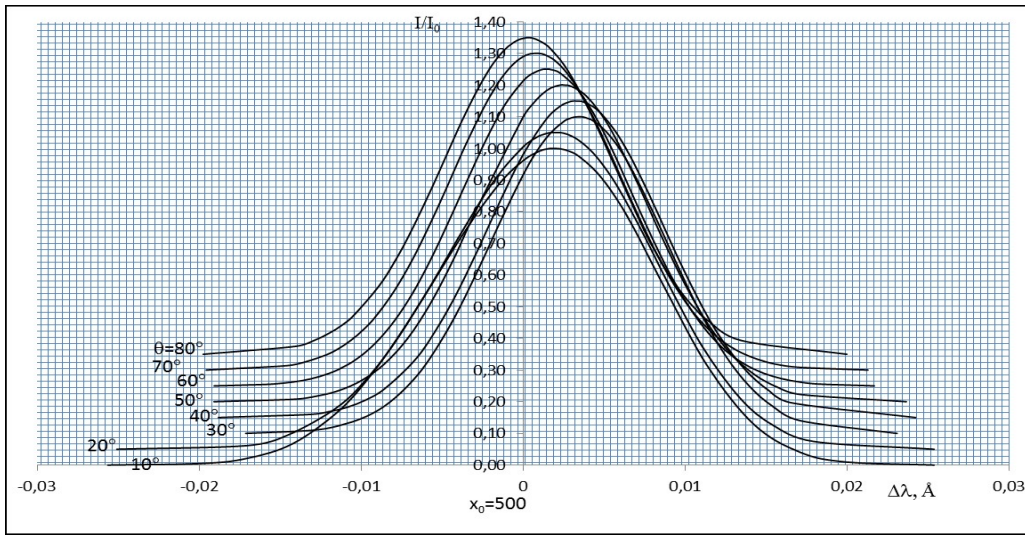

Fig. 2. Calculated profiles of the λ 171 FeIX line at different values of the angle of inclination of the line of sight ν for a wavelength Λ= 20,000 km. Profiles are calculated in units of center intensity. Profiles are displaced along the intensity axis.

account the results of our calculations. It should be noted that regarding the observed values of non-thermal velocities, there are few cases of determining ν_{nt} in the emission spectrum of slow magneto-sonic waves. Let us give examples of some of them.

The authors [28, 29], based on many coronal active region line observations, found the value of non-thermal velocities of 17 km/s and 10 km/s. Authors [30,31] found on the 171 Å line 7.5 km/s and 3 km/s, respectively. According to observations [32], in the Fe XIV 5303 line in the spectrum of slow waves, the velocity of Doppler shifts and non-thermal velocities are 0.3 km $s-1$ and 10-20 km s^{-1}, respectively. As can be seen, these values are in limits, obtained by us. The authors [24] observed the Doppler shift in coronal loops up to 300 km/s.

The authors consider that these are motions on slow magneto-sonic waves. However, the authors observed at the limb of the sun, in this case, the observations were carried out perpendicularly to the tube of the loop, and since slow sonic-wave propagates along the tube and motions on it occurring along the propagation, then the authors observed perpendicularly to the motions on the wave, and consequently, the observed motions cannot be motions on the slow magneto-sonic wave. Probably, the observed motions are motions on the bending wave. The authors [25] obtained v_d = 84 km/s; the observed wave is considered to be slow magneto-sonic wave. However, according to the authors' observations, there is a phase shift by 90° between density change n1 and velocity of motions on the

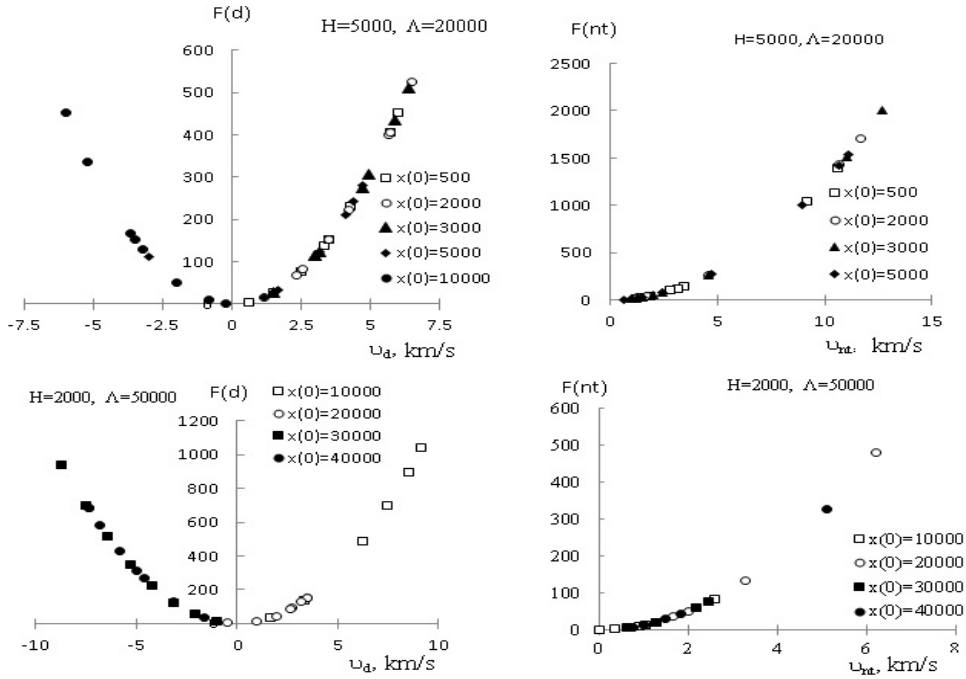

Fig. 3. Dependence of Energy flux density on Doppler shifts velocity (left) and non-thermal velocities obtained from Doppler width (right). Energy flux values in units $erg \cdot sm^{-2} \ldots^{-1}$

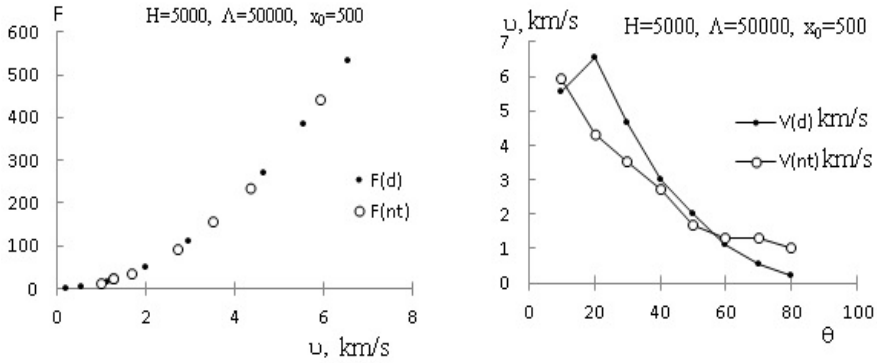

Fig. 4. Dependence of the energy flux density on Doppler shifts velocity (left) in erg $sm^{-2}s^{-1}$ and non-thermal velocities obtained from Doppler width (right) at specific values of the parameters.

wave v1; since density change means the intensity change, we can assert that the observed wave was standing slow magneto-sonic wave.

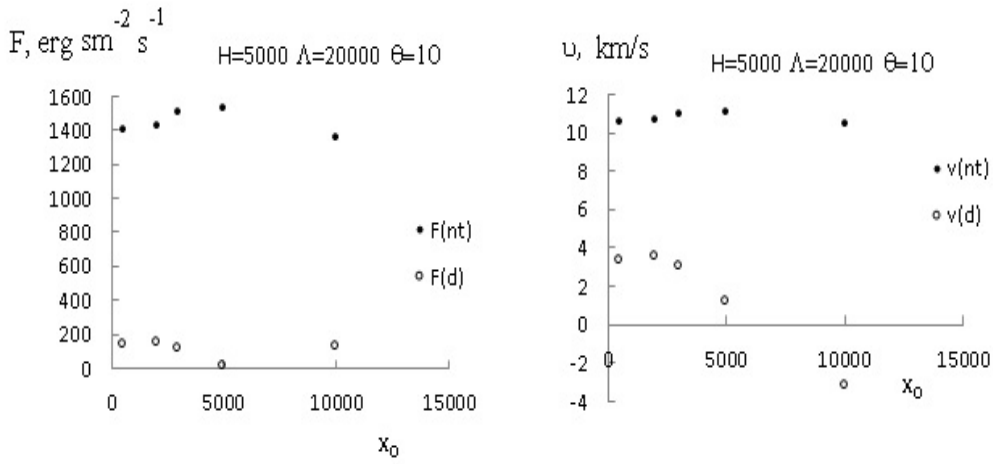

Fig. 5. DDependence of the energy flux density (left) and the phase velocities at θ = 10.

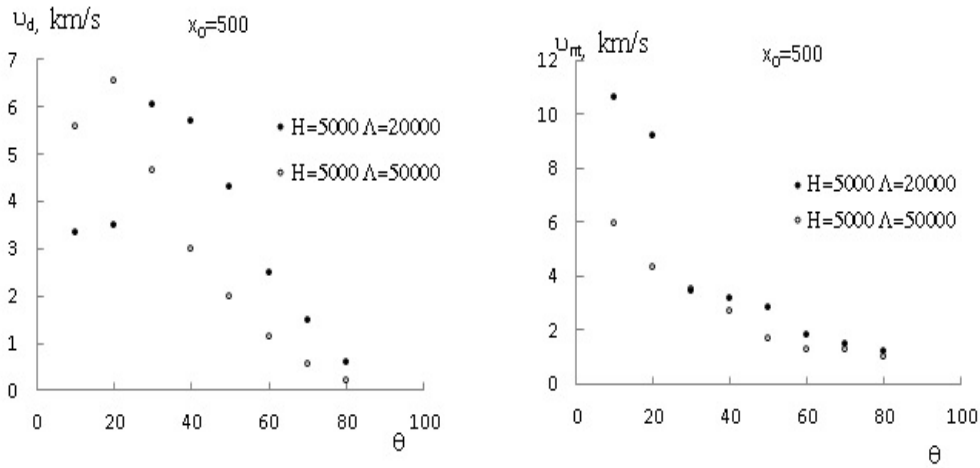

Fig. 6. Values of the Doppler shifts velocities ν_d and non-thermal velocities from the inclination angle θ at various wavelengths Λ and loop diameter H

Fig. 8 shows the dependence curves of the values of non-thermal velocities and the velocities of Doppler shifts depending on the angle of the line of sight, wave phase, wavelength, and the coronal loop's width. As can be seen from graphs, velocitie's values are changed from 12 km/s at small values of angle of sight to almost zero at large values of the angle of sight. The values of Doppler shifts at

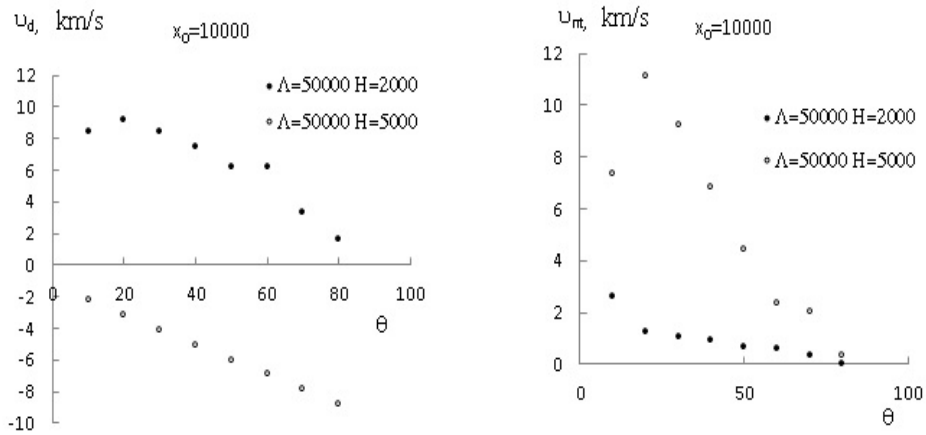

Fig. 7. Dependence of velocities on the angle of sight at indicated values of the parameters

large values of the angle of sight are close to the observed values, while at small values of angle of sight, our calculated values are mainly much higher than the observed ones. Apparently, it can be explained by the fact that the amplitude of the velocities on these waves is less than 10 km/s. As can be seen from Fig. 8, the velocities values depend on the loop width and wavelength.

Energy flux density. Fig.4 shows the dependence of the energy flux density on Doppler shifts velocity (left) in $sm^{-2}s^{-1}$ and non-thermal velocities obtained from the Doppler width (right) at specific values of the parameters. As shown in the figure, energy flux density increases with velocities increasing, which naturally, whereas with increasing of angle of sight θ to 100°, the flux density value decreases.

Fig. 5 shows the dependence of the energy flux density (left) and the phase velocities at $\theta = 10°$.

Fig. 3 shows the calculated values of the energy fluxes density depending on the Doppler shifts velocities and non-thermal velocities obtained from the Doppler widths of the calculated profiles at various values loop width H = 2000 km and 5000 km and wavelength Λ = 20,000 km and 50,000 km. The flux densities are calculated by the expression:

$$F = \frac{1}{2}\rho\nu^2\nu_{ph}$$

Here: ρ - density, the root-mean-square velocity of motions on the wave, ν_{ph} - phase velocity of the wave.

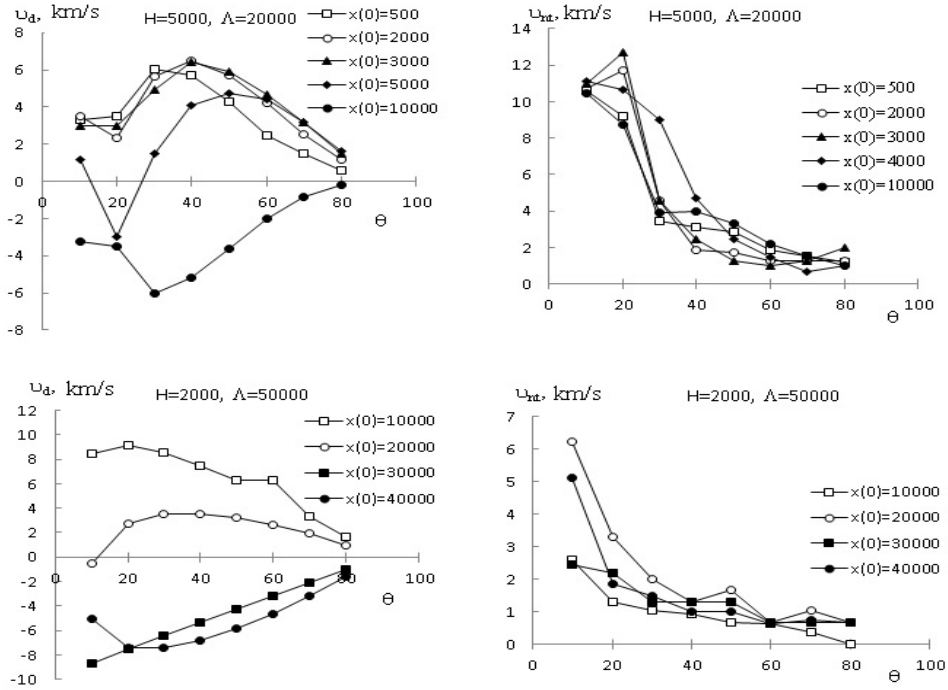

Fig. 8. Dependence of velocities on the angle of sight at various values of the phase

As can be seen from the figures, at values H = 5000 and Λ = 20000, the maximum value of F (nt) ($2{\cdot}10^3$ erg $sm^{-2}s^{-1}$) is almost five times greater than the maximum value of F (d) ($5.5 \cdot 10^5 ergsm^{-2}s^{-1}$).

Moreover, at the values of H = 2000 km and Λ = 50000 km, on the contrary, the maximum value of F (d) ($1 \cdot 10^3 erg\, sm^{-2}s^{-1}$) is almost two times greater than the maximum value of F (nt) ($5 \cdot 10^2 erg\, sm^{-2}s^{-1}$). This result shows that the flux values depend on the loop's width and the propagated slow sonic wavelength. The calculation of flux value for various values of the wave phase was performed. Fig. 3 shows how strongly the values of energy fluxes depend on the wave phase. The flux values at small values of the angle of sight vary from $2{\cdot}10^3 erg{\cdot}sm{-}2{\cdot}s^{-1}$ but at high values of the angle of sight almost to zero. It should be noted that the values at small angles of sight are close to observed ones [1–6]. The minimum value of Doppler shifts velocities and non-thermal velocities are $\sim$1 km/s and less; at this value, energy flux velocities are $\sim 10 - ergsm^{-2}s^{-1}$. It means that depending on the angle of sight ϑ and the wave phase, the observed energy flux values will differ by almost two orders of magnitude or more. However, an equal amount of energy flowing in the magnetic tube.This remarkable result can explain

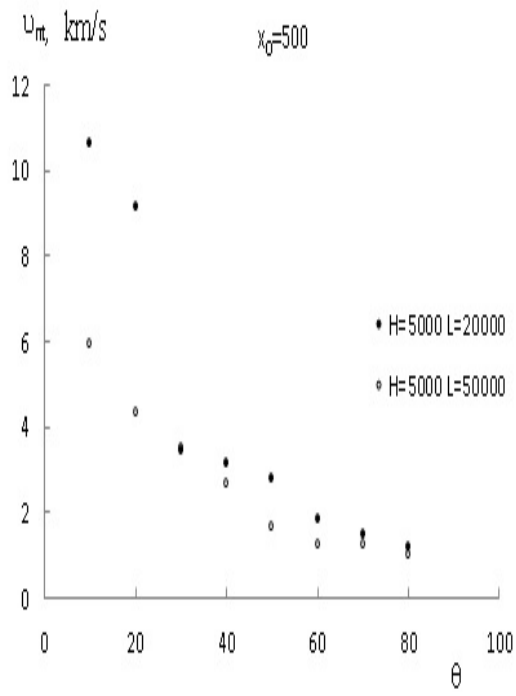

Fig. 9. Dependence of non-thermal velocities on the angle of sight at specified values of the parameters

the very different values of the energy flux of slow magneto-sonic waves obtained by various authors from observations [27].

The magnitude of the energy flux true value, calculated by the expression:

$$F = \frac{1}{4}\rho\nu_a^2\nu_{ph}$$

Calculated by the given value of the amplitude of velocities $\nu_a = 10$ km/s on the wave is erg $sm^{-2}s^{-1}$. An interesting result is that the calculated (observed) energy flux values can be significantly less or significantly more than the true value: from almost zero at small values of θ.

Asymmetry

Authors choose the area of certain wavelength interval on the profile at equal distances from the center of the line when studying the asymmetry in the emission lines of the mz wave. Line asymmetry is estimated by expression (R-B)/(R + B); here, R, B - the area's magnitude on red and blue sides from the center of the

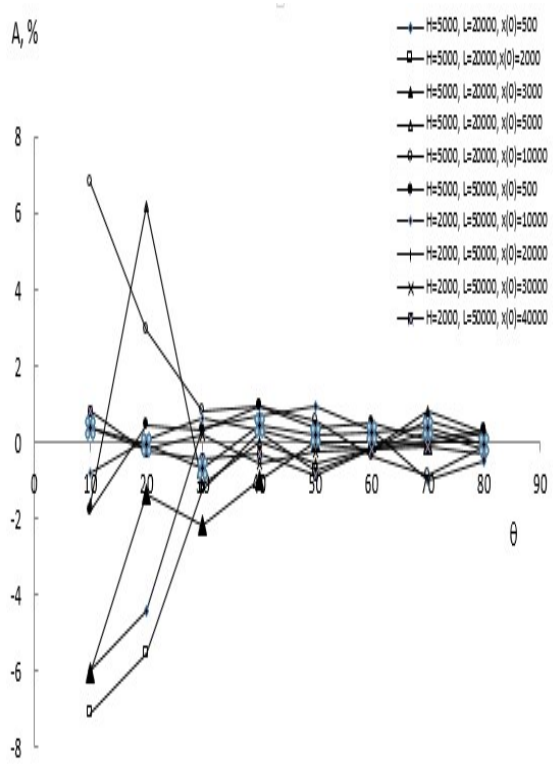

Fig. 10. Dependence of asymmetry on the angle of sight

line, respectively. It is conducted to reveal the presence of a possible flux of mass creating asymmetry [12].

We determined RB asymmetry over the entire wing of both blue (B) and red (R) since, in our case, the asymmetry is created by motions on the wave.

Almost in all works on determining the cause of the asymmetry of spectral lines, the authors conclude that the observed asymmetry is mainly blue, formed by plasma flow from below with velocities of 50–150 km/s [12, 18, 19]. In [19], the flux of mass from below is identified with spicules of type 2. In [26], the asymmetry is explained by the mass flux's quasiperiodic motion from below, which is superimposed on the mz wave.

The asymmetry values determined by us for all phases and wavelengths are shown in Fig. 10. As can be seen from the figure, at small values of the angle of the line of sight (ϑ>300), blue asymmetry is visible. At values of angle of sight ϑ>30° asymmetry is almost invisible. We can say that motions on the wave do not create asymmetry in the spectral line profile. It confirms the result obtained

from many author's observations that the flux of mass from below creates asymmetry, the emission profile of which is superimposed on the slow magneto-sonic wave's emission profile.

REFERENCES

1. De Moortel, I. and Nakariakov, V. M., 2012, "Magnetohydrodynamic waves and coronal seismology: an overview of recent results", Philos. Trans. R. Soc. London, Ser. A, 370, 3193–3216.

2. M.J. Aschwanden, Physics of the Solar Corona—An Introduction. (Praxis, Chichester, 2004). 1st Edition 2005 paperback

3. Nakariakov, V. M. & Verwichte, E. 2005 Coronal Waves and Oscillations. Living Reviews in Solar Physics, 2, 3.

4. De Moortel, I. 2005 An overview of coronal seismology. Royal Society of London . Philosophical Transactions Series A, 363, 2743–2760

5. De Moortel, I. 2006 Propagating magnetohydrodynamics waves in coronal loops. Royal Society of London Philosophical Transactions Series A, 364, 461

6. De Moortel, I. 2009 Longitudinal Waves in Coronal Loops. Space Science Rev.,149, 65–81.

7. McEwan M. P. and De Moortel I. 2006.: Longitudinal intensity oscillations observed with TRACE: evidence of fine –scale structure. A,A. v. 448, p. 763-773.

8. Devlen E, Zengin Çamurdan D. , Yardımçı and Pekünlü E.R.: A new model for heating of the Solar North Polar Coronal Hole. MNRAS, v.467, pp133-144

9. Porter L.J., Klimchuk J.A. and Sturrock P. A. 1994.: The role of MHD waves in heating of the Solar Corona. ApJ, v. 435, pp 482- 501.

10. De Moortel, A.W. Hood, J. Ireland and R. W. Walsh, 2002, Longitudinal intensity oscillations in coronal loops observed with trace. II. Discussion of Measured Parameters Solar Physics 209: 89–108.

11. S. Krishna Prasad, D. Banerjee, T. Van Doorsselaere, and J. Singh: «Omnipresent long-period intensity oscillations in open coronal structures». A&A 546, A50 (2012)

12. Verwichte E., Marsh M., Foullon C., Van Doorsselaere T., De Moortel I., Hood A.W. and Nakariakov A.M.: Periodic spectral line asymmetries in solar coronal structures from slow magnetoacoustic waves. ApJ, 2010, v. 724, p. L194- 198

13. B. John T. Mariska, Harry P. Warren, David R. Williams, and Tetsuya Watanabe, Observations Of Doppler Shift Oscillations With The Euv Imaging Spectrometer On Hinode The Astrophysical Journal, 681: L41–L44, 2008.

14. N. Kitagawa, T. Yokoyama, S. Imada, and H. Hara: Mode Identification Of Mhd Waves In An Active Region Observed With Hinode/Eis. Astrophysical Journal, 721:744–749, 2010

15. J. Threlfall, I. DeMoortel, S. W. McIntosh, and C. Bethge: First comparison of wave observations from CoMP and AIA/SDO. A&A 556, A124 (2013).

16. T.J. Wang, L. Ofman J.M. Davila, and J. T. Mariska Hinode/EIS observations of propagating low-frequency slow magnetoacoustic waves in fan-like coronal loops A&A 503, L25–L28 (2009)

17. T. J. Wang, S. K. Solanki, D. E. Innes, W. Curdt, and E. Marsch: Slow-mode standing waves observed by SUMER in hot coronal loops. A&A 402, L17–L20 (2003)

18. Bart De Pontieu, Scott W. McIntosh, Viggo H. Hansteen, and Carolus J. Schrijver: Observing The Roots Of Solar Coronal Heating—In The Chromosphere. Astrophysical Journal, 701:L1–L6, 2009

19. Scott W. McIntosh and Bart De Pontieu: High-Speed Transition Region And Coronal Upflows In The Quiet Sun. The Astrophysical Journal, 707:524–538, 2009.

20. John T. Mariska and K. Muglach: Doppler-shift, intensity, and density oscillations observed with the extreme Ultraviolet imaging spectrometer on hinod. ApJ, v. 713, p.573–583, 2010.

21. Curdt W., Wang T.J., Innes D.E., Solanki S.K., Damasch I. E., Kliem B. and Offman L: Dopler oscillations in hot coronal loops. ESA_SP-506,)), 2002.

22. Wang T.J., Solanki S.K.,Curdt W.,Innes D.E.and DammaschL.E.,: Oscilating Hot loops observed by sumer. 2002 ESASP.508.465W

23. E.C. Bruner, Jr.: Dynamics Of The Solar Transition Zone. The Astrophysical Journal, 226:1140-1146, 1978

24. O. Kjeldseth-Moe and P. Brekke: Time variability of active region loops observedwith. The coronal diagnostic spectrometer (cds) on soho. Solar Physics 182: 73–95, 1998

25. L. Ofman and Tongjiang Wang : Hot Coronal Loop Oscillations Observed By Sumer: Slow Magnetosonic Wave Damping By Thermal Conduction. Astrophysical Journal, 580:L85–L88, 2002

26. Bart De Pontieu, and Scott W. McIntosh: Quasi-Periodic Propagating Signals In The Solar Corona: The Signature Of Magneto-acoustic Waves Or High-Velocity Upflows. The Astrophysical Journal, 722:1013–1029, 2010.

27. Mamedov S. G. et al: About heating of the Solar Corona. AAJ, № 14, p.62, 2014.

28. David H.Brooks1,3 and Harry P.Warren:Measurments of non-thermal line widhts in solar active regions. The Astrophysical Journal, 820:63, 2016.

29. E. O'Shea1, D. Banerjee2, and J. G. Doyle1: A statistical study of wave propagation in coronal holes, A&A 463, 713–725 (2007).

30. L.Ofman V.M.Nakariakov and C.E.Deforest:slow magnetosonic waves in coronal plumes.The astrophysical journal,

31. I. De Moortel1, J. Ireland2, and R.W.Walsh1: Observation of oscillations in coronal loops. Astron. Astrophys. 355, L23–L26 (2000)

32. T.Sakurati,K.Ichimoto1,K.P.Raju2 and J.Singh2:Spectroscopic observation of coronalwaves.Solar Physics 209: 265–286, 2002